*Research Article*

# Personal Identification using the Distance and Triangle between the Metacarpophalangeal Joints

**Siwa Srathongkao[1], Yongyut Kaewjumras[2], Wanasanan Ngamsapmanee[1], Nuttakrit Somdock[1], Nalita Sawangjit[1] and Bhanupol Klongratog[1*]**

*Received: 29 August 2021*
*Revised: 8 April 2022*
*Accepted: 12 April 2022*

## ABSTRACT

Personal identification using the distance among the metacarpophalangeal joints (MCPs) was presented in this study. The system was developed to specify the dorsal hand patterns. Firstly, the dorsal hand images were taken for the subjects via an infrared camera. Secondly, the dorsal hand images were converted to grayscale and binary images using image processing techniques. After that, the distance of the MCPs was measured by various the dorsal hand images including index to middle, middle to ring, ring to little, and index to little of the dorsal hand. In addition, the triangle areas between index to middle, middle to ring, ring to little, and index to little of the dorsal hand were used to specify the dorsal hand patterns. The result of the distance and the triangle area of the MCPS can be used to identify a person because of the difference of distance and the triangle area of the MCPs of each person.

**Keywords**: Personal identification, Dorsal-hand, Metacarpophalangeal joint

[1]Department of Physics, Faculty of Science, King Mongkut's Institute of Technology Ladkrabang, Bangkok
[2]Department of Mechanical Engineering, Faculty of Engineering, Rajamangala University of Technology Srivijaya, Songkhla
*Corresponding author, email: bhanupol.kl@kmitl.ac.th

## Introduction

Normally, a fingerprint scan is required to assess the building. The same fingerprint scanner and face scanning technology are used on mobile phones and applications [1-4]. Nowadays, COVID-19 has spread in our country, and thus the fingerprint scanner and face scanning technology have a risk of contracting or spreading the COVID-19 virus. There are many researches that use the dorsal hand for identification. Benno Hartung used the hand vein pattern for identification purposes. The hand vein patterns of 30 study participants were analyzed from conventional frames of videography. A standardized grid system consisting of six lines and four sectors was applied to the dorsal of the hands. Vein branching within the sectors and line crossings of the veins were counted, leading to a total of 11 variables for each hand [5]. Jinfeng Yang used fingervein recognition refers to a recent biometric technique that exploits the vein patterns in the human finger to identify individuals [6]. Di Huang proposed a novel approach to hand dorsal vein recognition through matching local features of multiple sources [7]. The dorsal hand is an interesting way to examine the identity of the person because the person does not have to remove the masks or come into contact with tools or devices used to identify them. From the above, identification is recognized by visualizing the subcutaneous veins behind the hand and using the characteristics of each dorsal joint with fingers. However, the distance and triangular area of the metacarpophalangeal joint are of interest. There are specific features that can be used for identification. Therefore, we are interested in studying the relationship between the distance and the triangle area of the metacarpophalangeal joint [8].

## Materials and method

### Picture preparation

In this research, the dorsal hand image used images from Yildiz, MZ, et al. (2019) [9]. As shown in Figure 1, these are photographs of the dorsal hand taken by the image system consisting of an infrared camera (IR camera), a computer, an infrared filter (IR filter), and an infrared light source (IR source: 850 nm). When shooting the back of the hand with an infrared camera, the resulting image is then processed by converting the RGB image to a grayscale image, a binary image, and then image filters. To improve image quality (image enhancement) to obtain images with desired properties. Postfiltering images were used to determine the distance and triangle area of the metacarpophalangeal joint. The dorsal hand used in the processing will consist of images of 10 people, consisting of the image of the back of the right hand and images of the back of the left hand of 10 each. As shown in Figure 1, the captured image is converted from a color image (Figure 1a) into a 256-bit gray image (Figure 1b). Then a gray image is converted. A black-and-white image (Figure 1c) and image filtering (Figure 1d) were performed as a final step to improve image quality before finding the distance between the joints and the triangular area between the metacarpophalangeal joints.

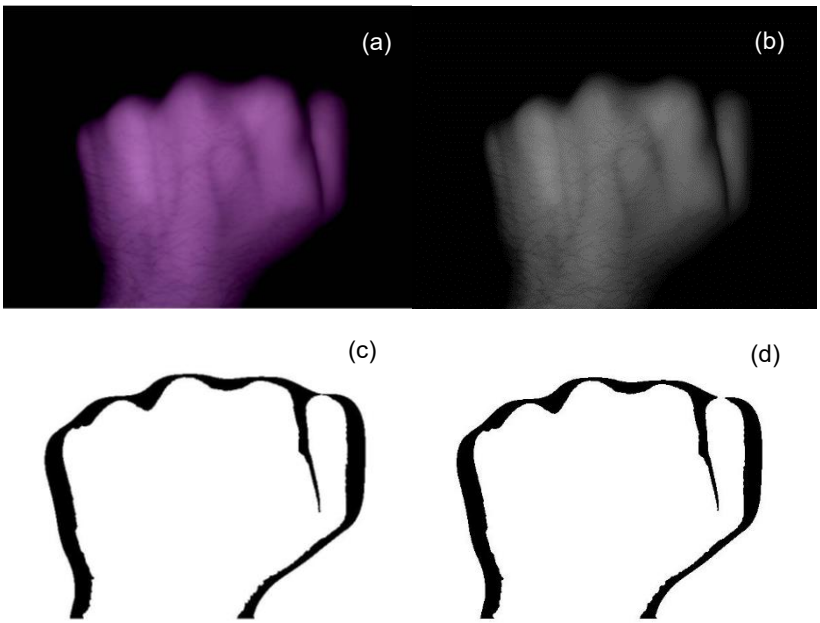


**Figure 1** The process of image processing after the hand (a) a color image, (b) a 256-bit gray image, (c) a black-and-white image and (d) image filtering.

**Image processing**

Image processing of the dorsal hand to determine the distance and triangular area between the metacarpophalangeal joints was performed using MATLAB. There are steps as follows: converting an RGB image to a grayscale image, converting a gray image to a binary image, filtering image data using median filtering, determination of the distance between the metacarpophalangeal joints, and finding the area of the triangle between the metacarpophalangeal joints [9].

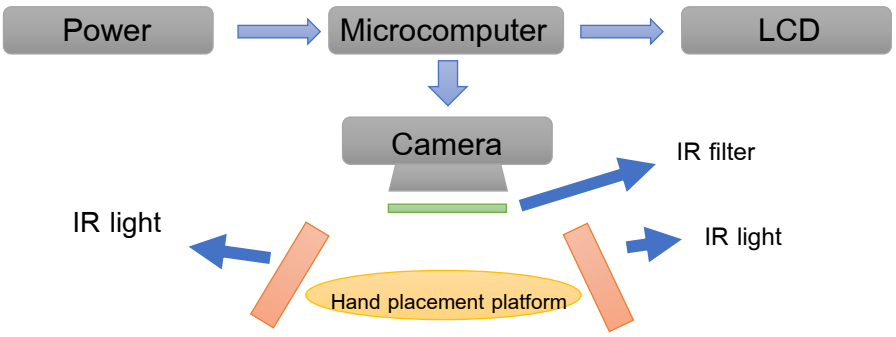


**Figure 2** Imaging system diagram.

**Converting an RGB image to a gray scale image**

A grayscale image is one in which the color intensity of each place in the image is represented by a number ranging from 0 to 255. The image contains a light-to-dark gradient that lies between white and black for an 8-bit grayscale image. Each pixel in an image represents the gray level intensity of

each pixel. Equation 1 [9] can be used to calculate the gray level value at the pixel to seek for.

$$A = (0.299 \times r) + (0.587 \times g) + (0.144 \times b) \quad (1)$$

where $A$ = The gray level value at the desired pixel point

$r$ = Red at the desired point

$g$ = Green at the desired point

$b$ = Blue at the desired point

**Converting a gray image to a binary image**

Binary images have just two potential intensities for each pixel. In terms of numbers, the two values are frequently 0 for black and 1 for white (Equation 2). The fundamental reason binary pictures are important in image processing is that they make it simple to distinguish an item from its surroundings. The segmentation technique allows us to designate each pixel as either "background" or "object" and assign black and white colors to each [10, 11].

$$B = \begin{cases} 0, & A < T \\ 2^c - 1 \end{cases} \quad (2)$$

where $B$ = The number of bits of the image system

$A$ = The light intensity of the image spot at the point under consideration

$c$ = The light intensity of the image spot in the same position after considering

$T$ = The threshold value

**Filtering image data using median filtering**

A nonlinear approach for removing noise from photos is median filtering, which is extensively used since it is quite good at reducing noise while keeping the edges. It is very good at getting rid of "salt and pepper" sounds. The median filter replaces each value with the median value of nearby pixels as it moves across the picture pixel by pixel. A nonlinear approach for removing noise from photos is median filtering, which is extensively used since it is quite good at reducing noise while keeping the edges. It is very good at getting rid of "salt and pepper" sounds. The median filter replaces each value with the median value of nearby pixels as it moves across the picture pixel by pixel. The "window" is the pattern of neighbors that glides pixel by pixel over the entire image, 2 pixels at a time. The median is derived by numerically ordering all the pixel values in the window and then replacing the pixel in question with the middle (median) pixel value other approaches with different properties that may be preferred in specific circumstances include the following: Avoid processing the boundaries, whether the signal or image boundary is cropped later. Obtaining data from other parts of the signal with photos for

example, entries from the far horizontal or vertical boundaries may be chosen reducing the size of the window at the edges so that each one is filled.

**Determination of distance between metacarpophalangeal joints.**

The first step is to determine the maximum coordinates for each of the metacarpophalangeal joints ($x_n$, $y_n$), which include the index, middle, and little fingers. Figure 3 depicts the coordinates. Equation 3 shows how to calculate the distance between the joints [11].

$$D = \sqrt{(x_{n+1} - x_n)^2 + (y_{n+1} - y_n)^2} \tag{3}$$

where $D$ = The distance between the metacarpophalangeal joints (mm)

$x_n, y_n$ = The starting point of the metacarpophalangeal joint (mm)

$x_{n+1}, y_{n+1}$ = The endpoint coordinate of the metacarpophalangeal joint (mm)

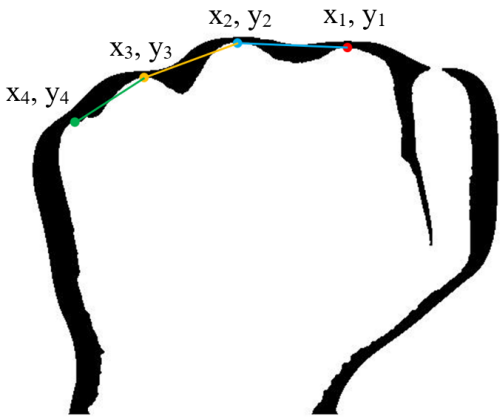


**Figure 3** Distance between metacarpophalangeal joints.

**Finding the area of the triangle between the metacarpophalangeal joints**

As illustrated in Figure 4, the area of the triangle can be found by measuring the distance between the coordinates on the x and y axes. Equation 4 may be used to calculate the triangle's area. The triangular area between the metacarpophalangeal joints of the index and middle fingers, the triangular area between the metacarpophalangeal joints of the middle and ring fingers, and the triangular area between the metacarpophalangeal joints of the ring and little fingers are the three parts of the metacarpophalangeal joints [11].

$$A = \frac{1}{2} \times |x_{n+1} - x_n| \times |y_{n+1} - y_n| \tag{4}$$

where $A$ = The area of the triangle $(mm)^2$

$x_n, y_n$ = The starting point of the metacarpophalangeal joint (mm)

$x_{n+1}, y_{n+1}$ = The endpoint coordinate of the metacarpophalangeal joint (mm)

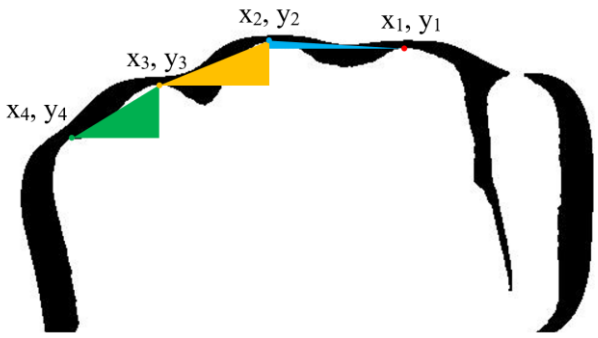


**Figure 4** Triangle area between metacarpophalangeal joints.

## Results

The distance between the forefinger and middle finger joints, the distance between the middle and ring finger joints, and the distance between the ring finger and little finger joints were all within the normal range in Table 1. Table 2 shows the distance between the right-hand metacarpophalangeal joints of ten individuals, which 9.7248, 5.0100, and 11.6103 mm were the differences, respectively. The differences between the middle finger, the distance between the middle and ring finger joints, and the distance between the ring finger and little finger joints were 8.7527, 11.0174, and 14.0315 mm, respectively, for the middle finger. The distance between the middle and ring finger joints, however, was different, as was the distance between the ring finger and little finger joints. It shows that when developed, the space between metacarpophalangeal joints may be utilized to identify or validate a person's identification.

**Table 1** Distance between joints in each joint of the left hand.

| Person | The distance between index and middle finger joints (mm) | The distance between middle and ring finger joints (mm) | The distance between the ring finger and little finger joints (mm) |
|---|---|---|---|
| 1 | 31.5254 | 26.8796 | 22.3256 |
| 2 | 24.9397 | 26.7870 | 19.8508 |
| 3 | 31.7026 | 24.0130 | 18.6958 |
| 4 | 31.5398 | 24.3718 | 25.9507 |
| 5 | 30.1996 | 23.7433 | 20.0316 |
| 6 | 33.7973 | 25.3683 | 30.3061 |
| 7 | 34.5674 | 27.5167 | 25.9157 |
| 8 | 34.6645 | 27.0290 | 20.6663 |
| 9 | 32.1988 | 28.3154 | 28.5186 |
| 10 | 29.3735 | 28.7533 | 21.5225 |

**Table 2** Distance between joints in each joint of the right hand.

| Person | The distance between index and middle finger joints (mm) | The distance between middle and ring finger joints (mm) | The distance between the ring finger and little finger joints (mm) |
|---|---|---|---|
| 1 | 31.0575 | 27.5942 | 23.4287 |
| 2 | 28.9691 | 24.7070 | 20.0979 |
| 3 | 28.3314 | 24.7099 | 22.7002 |
| 4 | 30.4719 | 35.2849 | 29.0476 |
| 5 | 30.6077 | 24.2675 | 24.3489 |
| 6 | 28.3314 | 29.2960 | 24.9355 |
| 7 | 37.0841 | 25.1145 | 22.0622 |
| 8 | 25.6987 | 24.9607 | 20.2350 |
| 9 | 28.5407 | 28.8214 | 27.3764 |
| 10 | 33.9503 | 29.1630 | 15.0161 |

Tables 3 and 4 show the triangular area determination of the posterior of the right and left hands at the metacarpophalangeal joint of the hand, where the triangular area consists of three components: the triangular area of the index and middle fingers; the area between the middle finger and ring finger; the area between the ring finger and little finger; and the triangular area between the index finger and middle finger joint; the triangle area between the middle finger and little finger. The differences were 315.3833, 304.2708, and 361.2888 $(mm)^2$, respectively, and the triangular area between the forefinger and middle finger joints, respectively, was 315.3833, 304.2708, and 361.2888 $(mm)^2$. On the left hand, the differences between the triangular areas between the middle finger and ring finger joints and the triangular areas between the ring finger and little finger joints were 691.4886, 412.0885, and 415.925 $(mm)^2$, respectively. When considering the triangular area of 10 individuals, both right- and left-handed, the area was different. It shows that the dorsal triangle area between the metacarpophalangeal joints can also be used to identify individuals.

**Table 3** The triangular area of the joints in each joint of the left hand.

| Person | The triangular area between the forefinger and middle finger joints $(mm)^2$ | The triangular area between the middle and ring finger joints $(mm)^2$ | The triangle area between ring finger and little finger joints $(mm)^2$ |
|---|---|---|---|
| 1 | 94.4562 | 452.4375 | 419.1000 |
| 2 | 87.0479 | 372.1364 | 250.0312 |
| 3 | 220.3979 | 329.9354 | 266.7000 |
| 4 | 110.1989 | 375.4437 | 413.8083 |
| 5 | 325.9667 | 253.2062 | 156.6333 |
| 6 | 350.0437 | 328.6125 | 355.6000 |
| 7 | 223.5729 | 508.0000 | 517.9218 |
| 8 | 34.6604 | 497.4167 | 244.7396 |
| 9 | 208.0948 | 557.4770 | 603.1177 |
| 10 | 218.2812 | 268.9490 | 291.5708 |

**Table 4** Triangle area of joints in each joint of the right hand.

| Person | The triangular area between the forefinger and middle finger joints $(mm)^2$ | The triangular area between the middle and ring finger joints $(mm)^2$ | The triangle area between ring finger and little finger joints $(mm)^2$ |
|---|---|---|---|
| 1 | 258.6567 | 347.3979 | 418.0417 |
| 2 | 257.1750 | 194.7333 | 202.8031 |
| 3 | 291.7031 | 252.8094 | 328.0833 |
| 4 | 571.5000 | 331.7875 | 517.7896 |
| 5 | 249.9320 | 318.3268 | 345.2812 |
| 6 | 64.1614 | 395.8167 | 314.8542 |
| 7 | 280.4583 | 402.8281 | 515.2760 |
| 8 | 755.6500 | 101.8646 | 101.8646 |
| 9 | 206.3750 | 513.9531 | 430.6094 |
| 10 | 291.7031 | 448.7333 | 364.9927 |

## Conclusion

The dorsal hand identification in this study uses the distance between the joints and the triangular area in the study to identify a person. Because the spacing and triangular area of the metacarpophalangeal joints are different, Tables 1 and 2 show the distances between the metacarpophalangeal joints. There are slight differences, so the triangular area between the metacarpophalangeal joints in Tables 3 and 4 is required to help identify the person. Then, the distance and triangular area between the metacarpophalangeal joints can be used for personal identification.

## Acknowledgements

The Department of Physics, Faculty of Science, King Mongkut's Institute of Technology Ladkrabang supported this research, and thanks to Yildiz, MZ, Boyraz, OF, Guleryuz, E., Akgul, A., and Hussain from the Department of Electrical & Electronics Engineering, Faculty of Technology, Sakarya University of Applied Sciences, 54187 Sakarya, Turkey, and the Department of Mathematics, Statistics, and Physics, Qatar University, Doha.

## References

1. Birngruber, C., Kreutz, K., Ramsthaler, F., Krähahn, J., & Verhoff, M. (2010). Superimposition technique for skull identification with Afloat® software. *International Journal of Legal Medicine*, *124*, 471–475.
2. De Boer, H., Blau, S., Delabarde, T., & Hackman, L. (2019). The role of forensic anthropology in disaster victim identification (DVI): recent developments and future prospects, *Forensic Sciences Research*, *4*(4), 303-315.
3. Valenzuela, A., Martín de las Heras, S. Marques, T., & Exposito, N. The application of dental methods of identification to human burn victims in a mass disaster. *International Journal of Legal Medicine*, *113*, 236-239.
4. Ferrer, M. A., Morales, A., & Ortega, L. (2009). Infrared hand dorsum images for identification. *Electronics Letters*, *45*, 306-308.
5. Travieso, C., Alonso, J. B., Briceno, J., & del Pozo-Baños, M. (2014). Hand shape identification on multirange images. *Information Sciences*, *275*, 45-56.
6. Chunyi, L., Mingzhong, L., & Xiao, S. (2012). A finger vein recognition algorithm based on gradient correlation. *AASRI Procedia*, *1*, 40-45.
7. Da Wu, J., & Huan Ye, S. (2009). Driver identification using finger-vein patterns with Radon transform and neural network. *Expert Systems with Applications*, *36*, 5793–5799.
8. Watanabe, M., Endoh, T. Shiohara, M., & Sasaki, S. (2005). Palm vein authentication technology and its applications. *Proceedings of the Biometric Consortium Conference*, 19-21 September 2005, Hyatt Regency Crystal City, Arlington, VA, USA.

9. Yildiz, M. Z., & Boyraz, O. F. (2019). Development of a low-cost microcomputer-based vein imaging system. *Infrared Physics & Technology*, *98*, 27-35.
10. Gonzalez, R. C., Woods, R. E., & Eddins, S. L. (2009). *Digital Image Processing Using MATLAB*. United States of America, Gatesmark Publishing a Division of Gatesmark, LLC.
11. Blanchet, G., & Charbit, M. (2006). *Digital Signal and Image Processing using MATLAB®*. Great Britain by Antony Rowe Ltd, Chippenham, Wiltshire.